CARBON 77 (2014) 518–524

Available at www.sciencedirect.com

ScienceDirect

journal homepage: www.elsevier.com/locate/carbon

Understanding the ultra-low friction behavior of hydrogenated fullerene-like carbon films grown with different flow rates of hydrogen gas

Yongfu Wang [a,b], Junmeng Guo [a,b], Kaixiong Gao [a], Bin Zhang [a], Aimin Liang [a], Junyan Zhang [a,*]

[a] State Key Laboratory of Solid Lubrication, Lanzhou Institute of Chemical Physics, Chinese Academy of Sciences, Lanzhou 730000, People's Republic of China

[b] School of Petrochemical Engineering, Lanzhou University of Technology, Lanzhou 730000, People's Republic of China

ARTICLE INFO

Article history:
Received 3 February 2014
Accepted 22 May 2014
Available online 5 June 2014

ABSTRACT

Fullerene-like hydrogenated carbon (FL-C:H) films that exhibit ultra-low friction and wear in humid conditions have been the subject of extensive researches, but the structure–performance relationship such as the evolution of FL structures under friction is not well understood. We have prepared FL-C:H films with different FL content, and have addressed a detailed investigation on the relationship. It is found that with the increase in FL content, the friction and wear of FL-C:H films can reach as low as 0.011 and 1.48×10^{-8} mm^3/Nm, respectively. Examination of the corresponding wear tracks by Raman spectroscopy reveals that not graphitization but friction-induced promotion of FL structures causes the ultra-low friction and wear of FL-C:H films. We therefore claim that FL structures are in close positive relations with the excellent tribological performance of FL-C:H films.

1. Introduction

The low friction combination with high wear resistance of amorphous carbon-based films has made their potential application in a wide range for material surface protection [1,2]. As it is known, the properties of materials are strongly dependent on their micro- and nanostructures. For amorphous carbon-based films, designing special nanostructures, such as fullerene-like (FL) [3–5], multilayer [6,7], and composite structures [8–10] provides other opportunities to significantly enhance material properties at the macroscale. In the past decades, FL carbon-based films, named for the presence of highly curved graphitic structures as in C_{60} fullerenes, have been the subject of extensive researches, due to their excellent mechanical and tribological properties. The FL structures consisting of bent, cross-linked, and frequently intersecting graphite sheets were first reported for graphitic carbon nitride (CN_x) [11] and later for pure carbon (C) films [12] and hydrogenated carbon (C:H) films [3,5]. In this study, fullerene-like hydrogenated carbon (FL-C:H) films that have shown unique ultra-low friction behavior in humid air are discussed. Structurally, the films are orderly and primarily made of sp^2-bonded carbon atoms. Chemically, they are made of carbon and hydrogen. Regarding their synthesis, they are mainly extracted from methane and/or hydrogen gases in a discontinuous and periodical discharged plasma growth environment by employing a high pulse bias [3,5].

* *Corresponding author:* Fax: +86 931 4968295.
E-mail addresses: topwyf8888@gmail.com (Y. Wang), zhangjunyan@licp.cas.cn (J. Zhang).

http://dx.doi.org/10.1016/j.carbon.2014.05.057
0008-6223/

Previous comparative tribological studies [5,13] with a-C:H and FL-C:H films revealed significant differences in their friction and wear behaviors in humid air environments. Specifically, the FL-C:H films were shown to provide a wide friction coefficient range (0.009–0.15) and long wear life, while the a-C:H films provided higher friction coefficients (i.e., as high as 0.4) and wore out quickly when tested in such environments. It seems that the lubrication of FL-C:H films stems from three-dimensional sp^2-based FL structures. However, the mechanism responsible for their lubricity is not well understood and scarcely reported; for example, how FL structures might evolve under friction? Are they graphitized? How the evolution might affect friction and wear behaviors of FL-C:H films? Additionally, a serious challenge of the comparative tribological studies is that in other studies, the friction coefficients of a-C:H films are measured to be in the similar range (0.02–0.20) [14] with FL-C:H films in humid environments.

In this study, we have prepared FL-C:H films with different FL content by varying flow rate of hydrogen gas and have provided a detailed investigation on the structure–performance relationship between FL structures and tribological features. Tribological behaviors of the FL-C:H films are obtained and discussed in terms of the ultimate sliding interfaces. The films with more FL structures exhibit lower friction. Especially, the films grown with the H_2 flow rate of 5 SCCM have the most FL structures and lowest friction and wear (0.011 and 1.48×10^{-8} mm^3/Nm) in humid air. Besides, Raman spectroscopies of corresponding wear tracks show one additional peak near 710 cm^{-1} that can be assigned to the curvature in graphitic planes and carbon nano-onions as has been confirmed in other reports. The Raman fitting results reveal that the odd ring fraction in the wear tracks is relatively higher than that of the original FL-C:H films, indicating that more FL structures generated in the tribological process. We therefore claim that the ultra-low friction and wear performances of FL-C:H films stem from their own unique FL structures, and not graphitization but friction-induced promotion of FL structures is responsible for excellent tribological performances.

2. Experimental

In this study, we used a direct current plasma chemical-vapor deposition (dc-PECVD) method to produce hydrogenated FL carbon films on Si (100) substrates. The films were about 500-nm thick and were derived from the mixed gases of methane and hydrogen. The deposition conditions were as follows: (1) applied dc negative voltage: 800 V; (2) gas flow rate: CH_4 = 10 SCCM, H_2 = 0, 2.5, 5, 7.5, and 10 SCCM. Further details of the deposition process can be found in [7]. The transmission electron microscopy (TEM) images and Raman spectra of as-deposited films were revealed by transmission electron microscope (FEI Tecnai F30, FEI, Eindhoven, The Netherlands) and Raman spectrometer (Jobin-Yvon HR-800, Horiba/Jobin Yvon, Longjumeau, France), respectively, with an excitation wavelength of 532 nm. For TEM analysis, about 20-nm-thick films grown under the above deposition conditions were produced on freshly cleaved NaCl wafers (single crystals), followed by dissolution of the NaCl substrate with distilled water and placed on Cu grids. No preparation treatments involving ion beams or chemical etching were used, which significantly reduced the possibility of introduction of microstructure artifacts. The chemical states of the films were determined using a PHI-5702 multifunctional X-ray photoelectron spectrometer (Physical Electronics Inc., USA) (XPS, operating with Al-Kα radiation and detecting chamber pressure of below 10^{-6} Pa). The friction behavior of the films against Al_2O_3 balls (Φ5) was assessed on a reciprocating ball-on-disc tribotester with a relative humidity (RH) of about 20%. All tests were performed under a load of 20 N, an amplitude of 5 mm, and a frequency of 12 Hz. In order to help in the interpretation, the a-C:H films were produced using the same deposition method (bias voltage 500 V, CH_4 30 SCCM, and working gas pressure 27 Pa) for comparison.

3. Results and discussion

3.1. Characteristics of the as-deposited FL-C:H films

The presence of FL structures within carbon-based materials is normally assessed by high resolution transmission electron microscopy (HRTEM). Fig. 1 shows the HRTEM plane-view images of the films deposited at different flow rates of H_2. It could be seen that the flow rate of H_2 has an obvious effect on the evolution of FL structures. The films grown with the H_2 flow rate of 0 SCCM exhibited a few straight and curved graphitic planes embedded in amorphous structures. The layer spacing was about 0.34 nm, which was in good agreement with the layer spacing of the graphite face (0002) [15]. With the increase in H_2 flow rate, more curved graphitic planes emerged, and these planes had large radii of curvature and formed parallel graphitic plane stacks about 2–3 nm in diameter. When the flow rate was increased from 5 to 10 SCCM, these typical FL features [15,16] were more clearly observed for the films. The HRTEM results proved evidently the formation of FL structures in hydrogenated carbon films prepared with a high flow rate of H_2.

Raman spectroscopy is an effective way to distinguish the microstructures of carbon films, especially, FL-C:H films. Usually, Raman spectrums of amorphous carbon films are characterized by a *G* peak around 1560 cm^{-1}, and a *D* shoulder peak around 1380 cm^{-1} [17]. Specially, for FL-C:H films, the Raman spectra can be well fitted by adding two extra peaks at approximately 1260 and 1470 cm^{-1} that are attributed to the curved graphitic structures [18–21]. Fig. 2 shows the Raman spectra of the films grown under different flow rates of H_2. First, these Raman spectrums showed a similar profile but a slight shifting of the *G* peak towards higher wave numbers with the increase in flow rate of H_2. The *G* peak shift was indicative for the increase of sp^2 content in these films. Second, as compared with the Raman spectra of typical hydrogenated amorphous carbon films, a weak peak around 1200 cm^{-1} was present in the Raman spectra. The peak was always accompanied with the appearance of FL structures, as had been confirmed by the Raman spectra in FL-CN_x[22] and FL-C:H films [3] Additionally, our films (in Fig. 1) showed curved graphitic sheets. So, according to the HRTEM and Raman results above, the Raman spectrums of the films deposited by dc plasma chemical vapor deposition were sim-

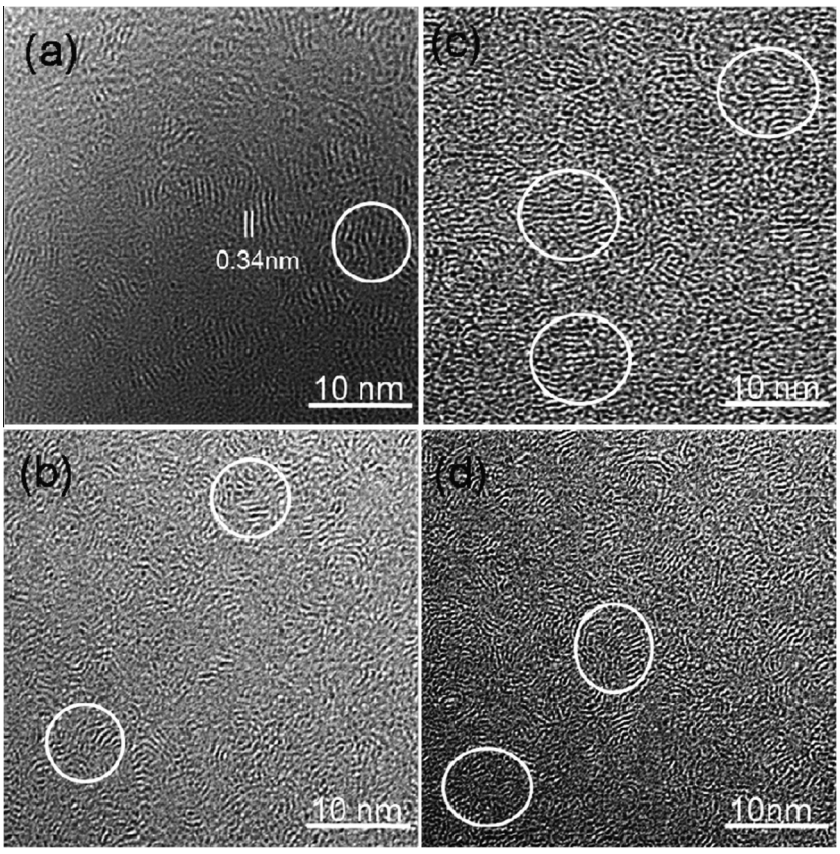

Fig. 1 – HRTEM micrographs of the as-prepared films under different gas flow rates of H_2. (a) 0 SCCM, (b) 2.5 SCCM, (c) 5 SCCM, and (d) 10 SCCM.

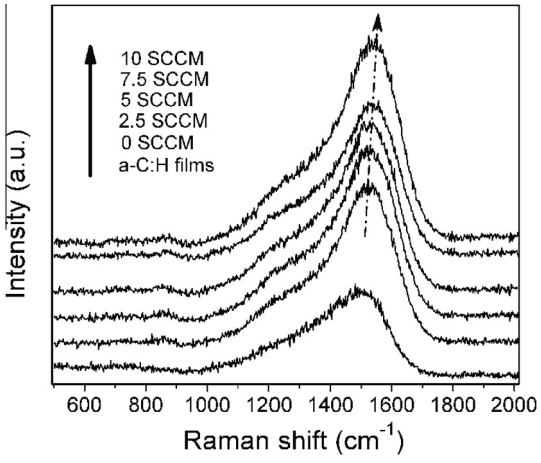

Fig. 2 – Raman spectra of fullerene-like hydrogenated carbon films grown with different gas flow rates of H_2.

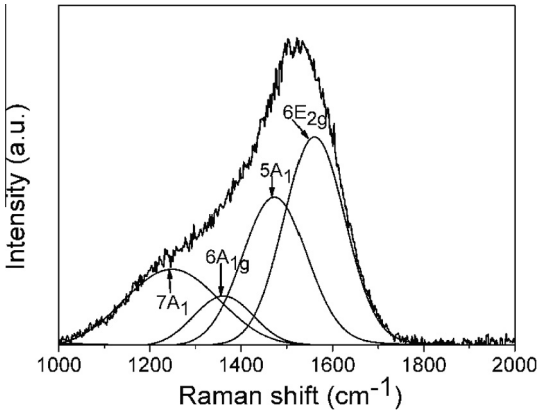

Fig. 3 – The fitted Raman spectra of fullerene-like hydrogenated carbon films grown with the H_2 gas flow rate of 5 SCCM.

ulated using four vibrational bands at 1248, 1362, 1473, and 1560 cm^{-1} (shown in Fig. 3) [18–21], three with A-type symmetry (from five-, six-, and seven-membered rings) and one with E-type symmetry (from six-membered rings). Fig. 4 shows the fractional contribution of each vibrational frequency to the Raman spectra as a function of the flow rate of H_2. As the flow rate increased, the fractions of $6E_{2g}$ did not show any obvious change, and the fraction of $7A_1$ was just on the opposite tendency with $6A_{1g}$. However, the fraction of $5A_1$ increased sharply when increased from 0 to 2.5 SCCM, decreased monotonously when increased to 7.5 SCCM, and increased sharply when at 10 SCCM. For pure carbon structures, according to the atomic modeling envisaged by Townsend et al. [23] and "squeezed chicken wire" model proposed by Alexandrou et al. [24] curvature and interlinking in purely sp^2-bonded structure can all take place through randomly oriented pentagonal and heptagonal rings or "defects." That is to say, the decrease or increase of the fraction of odd rings (five- and

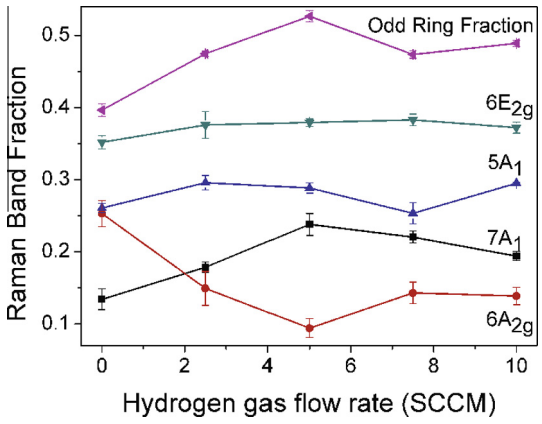

Fig. 4 – Contribution to the carbon Raman band from the vibrations of five-, six-, and seven-membered rings versus the gas flow rate of H_2. (A colour version of this figure can be viewed online.)

seven-membered rings) indicates the less or more curved graphite sheets and FL structures in the films with the increasing flow rate of H_2. Especially when increased to 5 SCCM, the films have the most odd ring fraction (Fig. 4), namely the most FL content.

We analyze the changes in these odd rings by considering the growth compressive stress, due to the bombardment of sufficiently energetic ions. The highly strained environment within depositing FL-C:H films will force plane curvature in an otherwise hexagonal structure, resulting in the evolution of both five- and seven-membered rings. In return, the creation of high pentatomic and heptatomic ring content easily leads to lower compressive stress of FL-C:H films (in a manner described elsewhere [21]). Before 5 SCCM, the promotion of odd rings originated from ion bombardment occurs along with the lower compressive stress; after 5 SCCM, the energetic ions, especially, more hydrogen atoms, which enter into the sublayer, cause higher compressive stress [2] and induce the hydrogenation of sp^2-bonded carbon, thus hindering the formation of odd rings in depositing FL-C:H films. So at 5 SCCM, a tipping point in structural changes is the result of the balance between the above two effects. However, when more hydrogen atoms enter into the sublayer, their excess energies are converted to thermal energies and then the energies diffuse outwards by thermal diffusion. In thermodynamics, pentatomic ring structures are more stable than heptatomic rings [25,26]. The pentatomic ring fraction consequently increases at 10 SCCM. But this does not mean that the six-membered ring fraction is decreasing (as shown in Fig. 4, the fractions of $6E_{2g}$ and $6A_1$ change slightly at 10 SCCM), only that newly formed π-bonds are grouping into pentatomic rings.

XPS was invoked for further investigation. The C 1s binding energies of pure graphite (284.3 eV) and diamond (285.3 eV) measured at the same conditions were cited for comparison. It could be seen that the C 1s core positions of the films grown with the H_2 flow rate of 0 and 5 SCCM were more adjacent to the C 1s position of graphite, than that of a-C:H films (Fig. 5). This result indicated that the films grown at 0 and 5 SCCM had a higher sp^2 content, and further proved that the films had FL structures.

3.2. *Friction behavior of FL-C:H films*

Fig. 6 shows the friction coefficients of the FL-C:H films as a function of sliding laps. All friction experimental results were repeatedly performed for more than three times. Figs. 7 and 8 present the friction coefficients, wear rates, and odd ring fraction as a gas flow rate of H_2. The friction coefficients and wear rates of the films changed in the opposite tendency of the fraction of odd rings with the increase in gas flow rate of H_2. In a word, the films with more FL structures exhibited lower friction and wear. Especially when increased to 5 SCCM, the friction coefficient of the films with the most odd ring fraction, namely the most FL structures, reached as low as about 0.011, and the wear rate was 1.48×10^{-8} mm^3/Nm in humid air. These results provide strong evidence to support the concept that ultra-low friction and wear of FL-C:H films originate from their own unique FL structures.

3.3. *Raman analysis on the wear track of FL-C:H films*

Although FL-C:H films exhibit ultra-low friction and wear under different conditions, the underlying tribological and wear mechanisms operating at the sliding interfaces are not fully understood yet. Buijnsters et al. [13] indicated that the lubrication mechanism of the films was in close positive relations with a "graphitized" tribofilm on the counter-wear surface. However, Zhang et al. [5] and Chen et al. [27] suggested that the curved graphitic planes could eliminate the energetic dangling bonds at the edge of the growing structure and thus permitted weak interactions at the sliding contact faces. In this study, we suggest that the ultra-low friction is caused by the promotion of FL structures in the tribological process. Fig. 9 shows the Raman spectrum taken at the centre of the wear track of FL-C:H films grown without H_2. As compared with the Raman spectra of original FL-C:H films (observed in Fig. 2), besides a weak peak around 1200 cm^{-1} originating from curved and cross-linked graphitic structures [3,22] and a peak at 850 cm^{-1} being related to amorphous SiC transition layer between the film and Si substrate [28,29], a low peak near 710 cm^{-1} appeared in the Raman spectrum. This peak

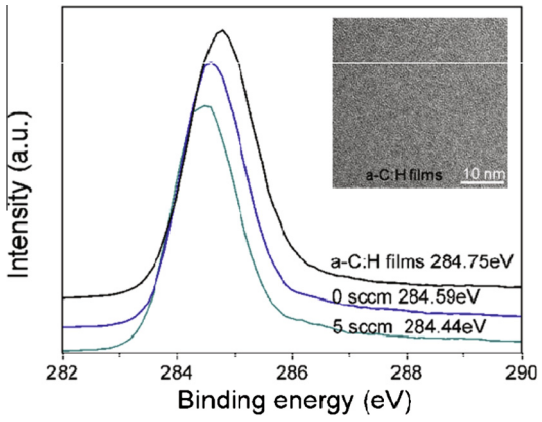

Fig. 5 – XPS C 1s peaks of a-C:H films and FL-C:H films grown with the H_2 flow rate of 0 and 5 SCCM. The inset shows HRTEM micrographs of a-C:H films. (A colour version of this figure can be viewed online.)

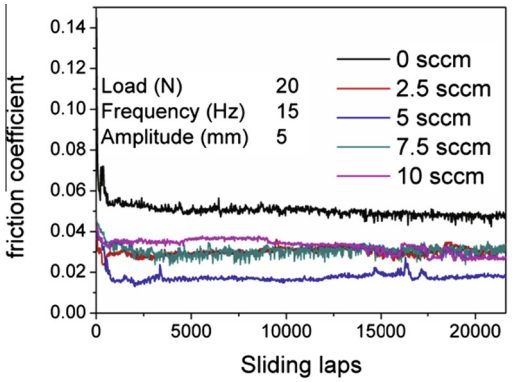

Fig. 6 – Friction coefficient of the FL-C:H films as a function of sliding laps in the same test environment. (A colour version of this figure can be viewed online.)

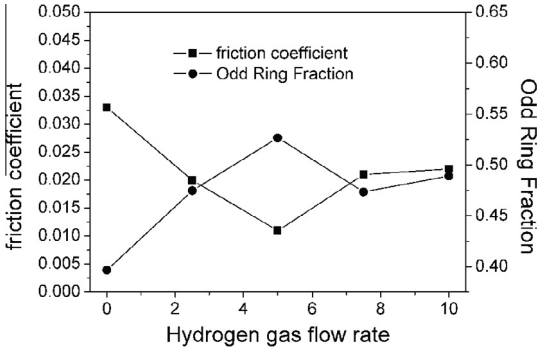

Fig. 7 – Friction coefficient and odd ring fraction of the FL-C:H films as a function of gas flow rate of H_2.

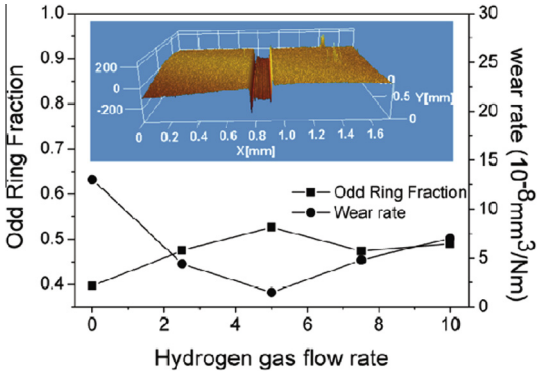

Fig. 8 – Wear rate and odd ring fraction of the FL-C:H films as a function of gas flow rate of H_2. The set shows 3D profiles of the wear tracks on the FL-C:H films grown with the H_2 flow rate of 5 SCCM. (A colour version of this figure can be viewed online.)

was previously observed in the Raman spectra acquired from the curvatures in graphitic planes and carbon nano-onions [3,30–33]. To further study the change in the bonding structures of the FL-C:H films in the tribological process, the Raman spectrum of the wear track in the range of 1000–2000 cm^{-1} was decomposed into four Gaussian peaks with wave numbers of about 1248, 1362, 1473, and

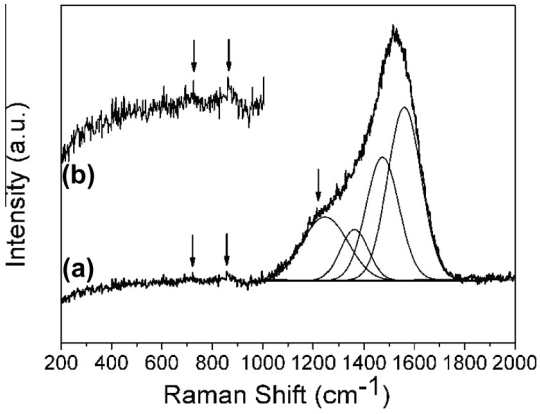

Fig. 9 – Raman spectrum taken at the centre of the wear track of FL-C:H film grown without H_2. (a) Raman spectra in the region from 1000 to 2000 cm^{-1} are deconvoluted into four peaks at 1248, 1362, 1473, and 1560 cm^{-1}. (b) Magnified wave number region from 200 to 1000 cm^{-1} in the Raman spectrum of (a).

1560 cm^{-1}. The odd ring fraction (~0.49) in the wear tracks was relatively higher than that (~0.40 in Fig. 7) of the original films. Combining with the preceding discussions (see Section 3.1), this higher odd ring fraction of the wear track indicated that more FL structures were generated in the tribological process. Similarly, the low peak near 710 cm^{-1} was more obviously observed in the Raman spectrum taken at the centre of the wear track of FL-C:H films, which was grown with the H_2 flow rate of 5 SCCM (Fig. 10) and had the lowest friction and wear (0.011 and 1.48×10^{-8} mm^3/Nm) in humid air. Furthermore, the wear track of the films had odd ring fraction of as high as ~0.61, more than that of its original films (~0.52 in Fig. 7). Herein, as discussed above, the additional peaks near 710 cm^{-1} and the higher odd ring fraction of the wear track indicated the friction-induced promotion of FL structures.

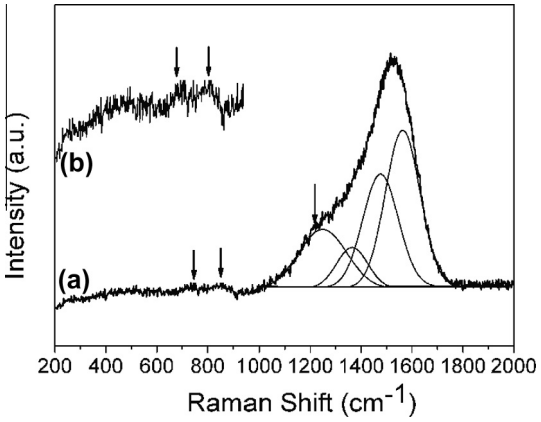

Fig. 10 – Raman spectrum taken at the centre of the wear track of FL-C:H film grown with the H_2 flow rate of 5 SCCM. (a) Raman spectra in the region from 1000 to 2000 cm^{-1} are deconvoluted into four peaks at 1248, 1362, 1473, and 1560 cm^{-1}. (b) Magnified wave number region from 200 to 1000 cm^{-1} in the Raman spectrum of (a).

However, the lubrication mechanism of the friction-induced promotion of FL structures is different from the "friction-induced graphitization" mechanism. The core of the graphitization mechanism is the increase of sp^2 content under friction, being regarded as the formation of crystalline graphite in amorphous carbon films [34]. Thus, weak van der Waals forces between the lamellar structures of graphite result in low friction. The mechanism still has two significant inadequacies: (1) these lamellar structures cannot be detected in graphitized layer by Raman spectroscopy [35–37], TEM [36,38], and electron-energy loss spectroscopy [36] and (2) the lamellar structures do not let graphite exhibit low friction in inert, dry, or even humid environments. However, the common characteristics of FL structures obtained in our FL-C:H films are the presence of graphitic atomic arrangements with in-plane curvature and the cross-link because of the presence of sp^3 carbon, but not the lamellar structures. Moreover, the FL-C:H films exhibit ultra-low friction and wear in humid conditions.

We expect that the preceding discussions will enrich the understanding of lubrication mechanism of FL-C:H films.

4. Conclusion

We have prepared FL-C:H films with different FL content by varying the flow rate of hydrogen gas. Tribological test showed that the films with more FL structures exhibited lower friction. Especially, the films grown with the flow rate of H_2 at 5 SCCM have the highest content of FL structures and the lowest friction and wear (0.011 and 1.48×10^{-8} mm^3/Nm) in humid air. The corresponding Raman spectroscopy of wear tracks showed one additional peak at 710 cm^{-1} and a higher odd ring fraction than that of original films, indicating that the promotion of FL structures in the tribological process. Our results provide strong evidence to support the concept that FL structures are in close positive relations with the excellent tribological performance of FL-C:H films.

Acknowledgment

This work is supported by the Major State Basic Research Development Program of China (973 Program) (No. 2013CB632304).

REFERENCES

[1] Lettington HA. Applications of diamond-like carbon thin films. Carbon 1998;36:555–60.
[2] Robertson J. Diamond-like amorphous carbon. Mater Sci Eng R 2002;37:129.
[3] Wang Q, Wang C, Wang Z, Zhang J, He D. Fullerene nanostructure induced excellent mechanical properties in hydrogenated amorphous carbon. Appl Phys Lett 2007;91:141902.
[4] Buijnsters JG, Camero M, Gago R, Landa-Canovas AR, Gómez-Aleixandre C, Jiménez I. Direct spectroscopic evidence of self-formed C60 inclusions in fullerenelike hydrogenated carbon films. Appl Phys Lett 2008;92:141920.
[5] Wang C, Yang S, Wang Q, Wang Z, Zhang J. Super-low friction and super-elastic hydrogenated carbon films originated from a unique fullerene-like nanostructure. Nanotechnology 2008;19:225709.
[6] Ager III JW, Anders S, Brown IG, Nastasi M, Walter KC. Multilayer hard carbon films with low wear rates. Surf Coat Technol 1997;91:91–4.
[7] Dwivedi N, Kumar S, Ishpal, Dayal S, Govind, Rauthan CMS, et al. Studies of nanostructured copper/hydrogenated amorphous carbon multilayer films. J Alloys Compd 2011;509(4):1285–93.
[8] Sarangi D, Sanjinés R, Karimi A. Enhancement of the mechanical properties of the carbon nitride thin films by doping. Carbon 2004;42(5–6):1107–11.
[9] Singh V, Palshin V, Tittsworth RC, Meletis EI. Local structure of composite Cr-containing diamond-like carbon thin films. Carbon 2006;44(7):1280–6.
[10] Wang A-Y, Lee K-R, Ahn J-P, Han JH. Structure and mechanical properties of W incorporated diamond-like carbon films prepared by a hybrid ion beam deposition technique. Carbon 2006;44(9):1826–32.
[11] Soo H, So S, Boman M, Sundgren J-E. Superhard and elastic carbon nitride thin films having fullerenelike microstructure. Phys Rev Lett 1995;75:1336.
[12] Amaratunga GAJ, Chhowalla M, Kiely CJ, Alexandrou I, Aharonov R, Devenish RM. Hard elastic carbon thin films from linking of carbon nanoparticles. Nature 1996;383:321.
[13] Buijnsters JG, Camero M, Vázquez L, Agulló-Rueda F, Gago R, Jiménez I, et al. Tribological study of hydrogenated amorphous carbon films with tailored microstructure and composition produced by bias-enhanced plasma chemical vapour deposition. Diamond Relat Mater 2010;19(7–9):1093–102.
[14] Ronkainen H, Holmberg K. Environmental and thermal effects on the tribological performance of DLC coatings. Tribology of diamond-like carbon films 2008;2:155.
[15] Neidhardt J, Hultman L, Czigány Z. Correlated high resolution transmission electron microscopy and X-ray photoelectron spectroscopy studies of structured CNx (0<x<0.25) thin solid films. Carbon 2004;42:2729–34.
[16] Alexandrou I, Kiely CJ, Papworth AJ, Amaratunga GAJ. Formation and subsequent inclusion of fullerene-like nanoparticles in nanocomposite carbon thin films. Carbon 2004;42(8–9):1651–6.
[17] Robertson ACFaJ. Interpretation of Raman spectra of disordered and amorphous carbon. Phys Rev B 2000;61:14095.
[18] Doyle T, Dennison J. Vibrational dynamics and structure of graphitic amorphous carbon modeled using an embedded-ring approach. Phys Rev B 1995;51:196–200.
[19] Siegal MP, Provencio PP, Tallant DR, Simpson RL, Kleinsorge B, Milne WI. Nanostructural study of the thermal transformation of diamond-like amorphous carbon into an ultrahard carbon nanocomposite. Appl Phys Lett 2000;76:2047.
[20] Siegal MP, Tallant DR, Martinez-Miranda LJ. Nanostructural characterization of amorphous diamondlike carbon films. Phys Rev B 2000;61:10451.
[21] Wang Q, He D, Wang C, Wang Z, Zhang J. The evolution of the structure and mechanical properties of fullerenelike hydrogenated amorphous carbon films upon annealing. J App Phys 2008;104:043511.
[22] Wang C, Yang S, Li H, Zhang J. Elastic properties of a-C:N: H films. J App Phys 2007;101:013501.
[23] Townsend SJ, Lenosky TJ, Muller DA, Nichols CS, Elser V. Negatively curved graphitic sheet model of amorphous carbon. Phys Rev Lett 1992;69:921.
[24] Alexandrou I, Scheibe HJ, Kiely CJ, Papworth AJ, Amaratunga GAJ, Schultrich B. Carbon films with an sp2 network structure. Phys Rev B 1999;60:10903.

[25] Siegal MP, Tallant DR, Provencio PN, Overmyer DL, Simpson RL, Martinez-Miranda LJ. Ultrahard carbon nanocomposite films. App Phys Lett 2000;76:3052.
[26] Sullivan JP, Friedmann TA, Baca AG. Stress relaxation and thermal evolution of film properties in amorphous carbon. J Electron Mater 1997;26:1021.
[27] Ji L, Li H, Zhao F, Quan W, Chen J, Zhou H. Effects of pulse bias duty cycle on fullerenelike nanostructure and mechanical properties of hydrogenated carbon films prepared by plasma enhanced chemical vapor deposition method. J Appl Phys 2009;105:106113.
[28] He XM, Walter KC, Nastasi M, Lee S-T, Fung MK. Investigation of Si-doped diamond-like carbon films synthesized by plasma immersion ion processing. J Vac Sci Technol A 2000;18:2143.
[29] Veres M, Koós M, Tóth S, Füle M, Pócsik I, Tóth A, et al. Characterisation of a-C: H and oxygen-containing Si:C: H films by Raman spectroscopy and XPS. Diamond Relat Mater 2005;14(3–7):1051–6.
[30] Roy D, Chhowalla M, Wang H, Sano N, Alexandrou I, Clyne TW, et al. Characterisation of carbon nano-onions using Raman spectroscopy. Chem Phys Lett 2003;373(1–2):52–6.
[31] Roy D, Chhowalla M, Hellgren N, Clyne TW, Amaratunga GAJ. Probing carbon nanoparticles in CNx thin films using Raman spectroscopy. Phys Rev B 2004;70:035406.
[32] Wang Z, Zhang J. Deposition of hard elastic hydrogenated fullerenelike carbon films. J Appl Phys 2011;109:103303.
[33] Blank VD, Buga SG, Dubitsky GA, Serebryanaya NR, Popov M Yu, Sundqvist B. High-pressure polymerized phases of C60. Carbon 1998;36:319.
[34] M'Ndange-Pfupfu A, Eryilmaz O, Erdemir A, Marks LD. Quantification of sliding-induced phase transformation in N3FC diamond-like carbon films. Diamond Relat Mater 2011;20(8):1143–8.
[35] Liu Y, Erdemir A, Meletis EI. A study of the wear mechanism of diamond-like carbon films. Surf Coat Technol 1996;82:48–56.
[36] Sánchez-Lópeza JC, Erdemir A, Donnetc C, Rojasa TC. Friction-induced structural transformations of diamondlike carbon coatings under various atmospheres. Surf Coat Technol 2003;163–164:444–50.
[37] Ambrosetti A, Ancilotto F, Silvestrelli PL. Van der waals-corrected ab initio study of water ice-graphite interaction. J Phys Chem C 2013;117(1):321–5.
[38] Merkle AP, Erdemir A, Eryilmaz OL, Johnson JA, Marks LD. In situ TEM studies of tribo-induced bonding modifications in near-frictionless carbon films. Carbon 2010;48(3):587–91.